ISSN 1070-3284, Russian Journal of Coordination Chemistry, 2018, Vol. 44, No. 12, pp. 806–811. © Pleiades Publishing, Ltd., 2018.

Halide Anion Templated Synthesis and Structural Characterization of Rhombic Dodecahedron Silver-Alkynyl Cage Complexes[1]

Z. N. Liang[a], X. M. Li[a], Z. Y. Zhang[a, *], Z. Y. Yu[a], and R. Cao[a, b]

[a] *Department of Chemistry, Renmin University of China, Beijing, 100872 P.R. China*

[b] *School of Chemistry and Chemical Engineering, Shaanxi Normal University, Xi'an, Shaanxi, 710119 P.R. China*

**e-mail: zhangzongyaochem@ruc.edu.cn*

Received March 21, 2018

Abstract—A series of silver alkynyl cages were synthesized using ligand 3,5-di-*tert*-butyl-phenylethynide and were structurally characterized. Reaction with $[Ag(ArC{\equiv}C)]_n$ polymer and $(^nBu_4N)X$ (X = F, Cl, Br) gave compounds incorporating different halogen anions (F^-, Cl^-, Br^-) and a hollow compound, namely $[Ag_{14}(ArC{\equiv}C)_{12}(MeCN)_6](OTf)_2 \cdot 4MeCN$ (**I**), $[Ag_{14}(ArC{\equiv}C)_{12}(EtOH)_2F]F \cdot EtOH$ (**II**), $[Ag_{14}(ArC{\equiv}C)_{12}(THF)_2Cl]OH \cdot THF$ (**III**) and $[Ag_{14}(ArC{\equiv}C)_{12}(MeCN)_4Br]OH$ (**IV**) (ArC≡C = 3,5-di-*tert*-butyl-phenylethynide). Direct synthesis of anion containing cages and indirect synthesis from the hollow cage were achieved. Structural studies (CCDC nos. 1831128 (**I**), 1831129 (**II**), 1831130 (**III**), and 1831131 (**IV**)) revealed that the incorporation of anions reduced the mean Ag–Ag bond length and therefore the cage size, giving the order of $F@Ag_{14} \approx Cl@Ag_{14} < Br@Ag_{14} <$ halogen-free. The cage size was larger than those of similar Ag_{14} clusters reported previously, which is likely due to the use of bulky alkynyl ligands.

Keywords: silver(I), alkynyl ligands, cage complexes, template synthesis, anions, crystal structures

DOI: 10.1134/S1070328418120059

INTRODUCTION

Silver acetylides are a large family of organometallic complexes, which have attracted extensive research interests because of their intriguing structural features [1] and their potential applications in catalysis [2–6] and material sciences [7–9]. On one hand, silver acetylides are among the oldest organometallics known [10]. More importantly, they provide a fascinating system for self-assembly of coordination polymers or convergent metal clusters through diverse coordination modes between silver salts and ethynide ligands abetted by the metallophilic interaction of d^{10} metal centers [10]. However, despite these achievements, owing to its inherence polymeric nature, structural characterization of silver acetylides is still a challenge and on most occasions [11]. Silver acetylides are not soluble in common solvent and aggregate and precipitate immediately upon formation. Silver acetylides are also synthons and fundamental building blocks for the construction of larger silver cluster even frameworks [12–14]. For all these reasons, structural studies of silver acetylides are the subject of great significance.

According to previous synthetic reports, extra amounts of $AgBF_4$ or other Ag(I) salts had to be added in order to improve the solubility, preventing the desired product from aggragating and precipitating upon formation [10, 15]. One way to solve this problem is to develop new methods to grow crystals. Recently, our group developed a robust and accessible counter diffusion microfluidic device and used it to synthesize and grow crystals of organometallic polymers that are not soluble for crystallization using traditional methods [16]. We get single crystals of X-ray diffraction quality of silver phenylacetylide and determine its structure unambiguously. It is the first single-crystal X-ray structure of silver phenylacetylide. Another way to improve the solubility of silver acetylides is to modify the alkynyl ligand. By using the 3,5-di-*tert*-butyl-phenylethynide (ArC≡C) ligand, we synthesize and get suitable single-crystals for X-ray diffraction of all-alkynyl-stabilized silver acetylides $[Ag(ArC{\equiv}C)]_n$, which have high solubility in nonpolar organic solvents, such as dichloromethane, chloroform, toluene, and even diethyl ether [17]. The new phenylethynide ligand with two sterically bulky *tert*-butyl substituents can confine the metal core to a certain size by preventing infinite aggregation of Ag metals. The crucial role of ArC≡C in the construction and stabilization of high-nuclearity Ag clusters motivated us to apply this ligand to synthesize mixed alkynyl Au–Ag clusters and get an all-alkynyl-stabilized $[Au_8Ag_8(ArC{\equiv}C)_{16}]$ cluster [18].

However, the previous work did not include anion templates, since it was an important way to form high

[1] The article is published in the original.

cores metal clusters [7, 14, 19]. In order to have a further understanding of the role of anions in clusters, we reported the synthesis and structural characterization of a series of silver cages by using ArC≡C ligand and halogen anions as template. These complexes are $[Ag_{14}(ArC{\equiv}C)_{12}(MeCN)_6](OTf)_2 \cdot 4MeCN$ (**I**), $[Ag_{14}(ArC{\equiv}C)_{12}(EtOH)_2F]F \cdot EtOH$ (**II**), $[Ag_{14}(ArC{\equiv}C)_{12}(THF)_2Cl]OH \cdot THF$ (**III**), and $[Ag_{14}(ArC{\equiv}C)_{12}(MeCN)_4Br]OH$ (**IV**). Structures of the four complexes contain fourteen silver atoms and twelve ligands, wherein the silver atoms constitute a rhombic dodecahedron cage. There is no anion in the silver cage of complex **I**, while F^-, Cl^- and Br^- anions are placed in the silver cage of complex **II**, **III** and **IV**. The analysis of the structures reveals that the halogen anions have significant influence on the formation of the structures.

EXPERIMENTAL

Methods and materials. Manipulations of air- and moisture-sensitive materials were performed under nitrogen gas using standard Schlenk line techniques. 3,5-di-tert-butylphenylethynide and its corresponding silver acetylide complex $[Ag(ArC{\equiv}C)]_n$ were synthesized according to published methods [17]. All other reagents were purchased from commercial suppliers and used as received unless otherwise noted. Dry solvents, including MeCN, THF, EtOH and DCM were purified by passage through activated alumina.

Electronic absorption spectra were acquired on a Cary 50 spectrophotometer. Infrared spectra (2% sample in KBr pellet) were recorded using a Bruker spectrophotometer with the OPUS software. ESI^+-MASS measurements were performed on a Bruker Fourier transform ion cyclotron resonance mass spectrometer APEX IV. Powder X-ray diffraction (PXRD) patterns were recorded at room temperature on a Shimadzu PXRD-7000 diffractometer (CuK_α, 40 kV and 40 mA).

Synthesis of complex I. A sample of $[Ag(ArC{\equiv}C)]_n$ polymer (2 mmol, 680 mg) was dissolved in 6 mL of DCM. To this solution, AgOTf (2 mmol, 514 mg) dissolved in MeCN (12 mL) was added under vigorous stirring. A colorless solution formed immediately. After 3 h, the solvent was evaporated. The resulting white solid was dissolved with MeCN, and the solution was filtered. Slow evaporation of the clear colorless solution afforded complex **I** as crystalline colorless blocks. The yield was 580 mg (90%). IR (ν, cm^{-1}): 2045 $\nu_m(C{\equiv}C)$.

For $C_{214}H_{282}N_{10}O_6F_6S_2Ag_{14}$

Anal. cacld., %	C, 56.92	H, 6.33	N, 1.95
Found, %	C, 56.90	H, 6.34	N, 1.96

Synthesis of complex II. A sample of $[Ag(ArC{\equiv}C)]_n$ polymer (2 mmol, 680 mg) was dissolved in 6 mL of DCM. To this solution, AgOTf (2 mmol, 514 mg) dissolved in MeCN (12 mL) was added under vigorous stirring. A colorless solution formed immediately. Then $(^nBu_4N)F$ (0.14 mmol, 36.6 mg) dissolved in EtOH (2 mL) was added dropwise, the solution still clear and colorless, 5 h later, the solution was filtered, slow evaporation of the solution afforded the complex **II** as crystalline colorless blocks.

IR (ν, cm^{-1}): 2045 $\nu_s(C{\equiv}C)$. MS (ESI) (*m*/*z*): 4073.1603 $[Ag_{14}(ArC{\equiv}C)_{12}F]^+$, 3433.0215 $[Ag_{12}(ArC{\equiv}C)_{10}F]^+$, 2027.3215 $[Ag_7(ArC{\equiv}C)_6]^+$.

For $C_{200}H_{276}O_4F_2Ag_{14}$

Anal. cacld., %	C, 55.96	H, 6.48
Found, %	C, 54.59	H, 6.22

Synthesis of complex III. $(^nBu_4N)Cl$ (0.14 mmol, 38.9 mg) was added to a mixture of $[Ag(ArC{\equiv}C)]_n$ polymer (2 mmol, 680 mg) and AgOTf (2 mmol, 514 mg) in THF (15 mL). After stirring the mixture for 5 h, the solvent was filtered, slow evaporation of the solution afforded complex **III** as crystalline colorless blocks.

IR (ν, cm^{-1}): 2045 $\nu_s(C{\equiv}C)$. MS (ESI) (*m*/*z*): 4089.6119 $[Ag_{14}(ArC{\equiv}C)_{12}Cl]^+$, 3449.4731 $[Ag_{12}(ArC{\equiv}C)_{10}Cl]^+$, 2027.3215 $[Ag_7(ArC{\equiv}C)_6]^+$.

For $C_{204}H_{277}O_4ClAg_{14}$

Anal. cacld., %	C, 56.47	H, 6.43
Found, %	C, 54.52	H, 6.25

Synthesis of complex IV. $(^nBu_4N)Br$ (0.14 mmol, 45.1 mg) was added to a mixture of $Ag(ArC{\equiv}C)]_n$ polymer (2 mmol, 680 mg) in DCM and AgOTf (2 mmol, 514 mg) in MeCN. After stirring the mixture for 5 h, the solvent was filtered, slow evaporation of the solution afforded complex **IV** as crystalline colorless blocks.

IR (ν, cm^{-1}): 2045 $\nu_m(C{\equiv}C)$. MS (ESI) (*m*/*z*): 4134.0659 $[Ag_{14}(ArC{\equiv}C)_{12}Br]^+$, 3493.9271 $[Ag_{12}(ArC{\equiv}C)_{10}Br]^+$, 2027.3215 $[Ag_7(ArC{\equiv}C)_6]^+$.

For $C_{200}H_{264}N_4OBrAg_{14}$

Anal. cacld., %	C, 55.47	H, 6.15	N, 1.29
Found, %	C, 55.52	H, 6.21	N, 1.31

X-ray diffraction analysis. The data of four single crystals were collected on a Bruker D8 VENTURE X-ray diffractometer performing φ- and ω-scans at 150(2) K. Diffraction intensities were measured using graphite monochromated MoK_α radiation (λ = 0.71073 Å). Data collection, indexing, initial cell

Table 1. Crystallographic data and structure refinements for **I**–**IV**

Parameter	Value			
	I	**II**	**III**	**IV**
Formula weight	4778.80	4292.39	4537.98	4330.24
Temperature, K	150(2)	153(2)	150(2)	150(2)
Crystal system	Triclinic	Triclinic	Triclinic	Triclinic
Space group	$P\bar{1}$	$P\bar{1}$	$P\bar{1}$	$P\bar{1}$
a, Å	19.4389(16)	15.9764(13)	19.651(2)	15.9294(15)
b, Å	20.0613(18)	18.8734(16)	20.264(2)	19.0977(18)
c, Å	34.311(3)	21.5234(18)	30.800(3)	19.9981(18)
α, deg	93.084(3)	80.774(2)	92.009(3)	65.215(3)
β, deg	103.970(2)	68.481(2)	91.832(3)	75.650(3)
γ, deg	117.003(2)	82.714(2)	91.983(3)	82.543(3)
V, Å^3; Z	11360.6(17); 2	5943.1(9); 1	12244(2); 2	5348.7(9); 1
ρ_{calcd}, Kg/m^3	1.397	1.199	1.231	1.344
μ, mm^{-1}	1.251	1.167	1.149	1.481
θ Range for data collection, deg	2.15–26.43	2.25–26.46	2.16–25.35	2.23–24.71
Reflections collected/unique	228629/46577	48824/23915	190258/44597	63503/17770
R_{int}	0.0349	0.0683	0.0548	0.0925
GOOF on F^2	1.030	1.044	1.028	1.039
Final R indices ($I > 2\sigma(I)$)	$R_1 = 0.0580$ $wR_2 = 0.1682$	$R_1 = 0.0823$ $wR_2 = 0.2420$	$R_1 = 0.1056$ $wR_2 = 0.2908$	$R_1 = 0.1007$ $wR_2 = 0.2479$
R indices (all data)	$R_1 = 0.0775$ $wR_2 = 0.1836$	$R_1 = 0.1616$ $wR_2 = 0.2828$	$R_1 = 0.1535$ $wR_2 = 0.3373$	$R_1 = 0.1662$ $wR_2 = 0.2993$
Largest peak and deepest hole, e Å^{-3}	4.392 and –2.867	2.302 and –0.943	2.192 and –2.169	1.725 and –4.086

refinements, frame integration and final cell refinements were accomplished using the program APEX2 [20]. Data reduction and empirical absorption correction were performed using the SAINT and SADABS program [20]. The structures were solved by the direct method using SHELXS [21] and refined by full-matrix least squares F^2 using SHELXL [21]. Crystal data, data collection and structure refinement details were summarized in Table 1.

Supplementary material for structures has been deposited with the Cambridge Crystallographic Data Centre (CCDC nos. 1831128 (**I**), 1831129 (**II**), 1831130 (**III**) and 1831131 (**IV**); deposit@ccdc.cam.ac.uk or http://www.ccdc.cam.ac.uk).

RESULTS AND DISCUSSION

Depending on the anions, there are four different structures reported. As initially observed, the Ag_{14} cage has the shape of rhombic dodecahedron (Fig. 1). However, the relatively low symmetry properties make it lack the 3-fold rotational axis that a regular rhombic dodecahedron should have. Overall, all of these structures own more than 3 types of silver atoms and has the same crystallographic i and molecular i symmetries. Commonly the silver atoms in the structure are arranged in 3 layers with 6 Ag(I) in the center layer and 4 Ag(I) in the side layer, forming a near-regular rhombic dodecahedron cage. And there are twelve ArC≡C ligands surrounded to support the cationic cage. Also, there are several solvent molecules in the structures, and complexes **II**, **III**, and **IV** have an anion in the geometric center of the cage. Though these silver cages are similar to each other, there are still some differences in the coordination modes of the alkynyl ligand. In the crystal lattice of complex **I**, there are ten alkynyl ligands taking the μ_3-η^1, η^1, η^1 mode, and two ligands are in μ_5-η^1, η^1, η^1, η^2, η^2 coordination mode. For complexes **II** and **IV**, though ten ligands are bound to the silver atoms in μ_3-η^1, η^1, η^1 mode, the other two ligands are in μ_4-η^1, η^1, η^1, η^2 mode. Different from the structure of complexes **I**, **II**, and **IV**, in the structure of complex **III**, twelve ArC≡C ligands all take the coordination mode of μ_3-η^1, η^1, η^1, and each pair of alkynyl groups are almost linearly bonded to each capped silver atom, and every ligand bridges two nearby silver atoms on each edge of the cube.

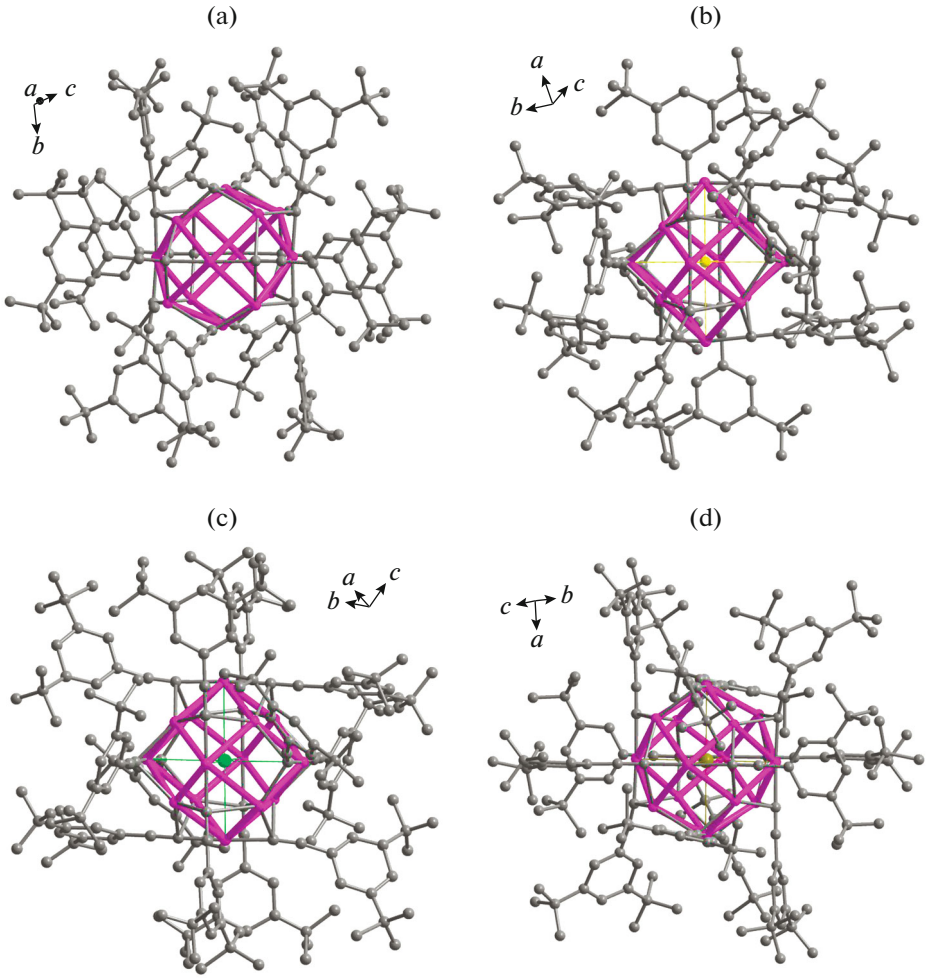

Fig. 1 Crystal structures of complexes **I** (a), **II** (b), **III** (c), and **IV** (d). Solvent molecules and hydrogen atoms are omitted for clarity.

Herein, we concluded the Ag anion distances (Table 2). The Ag anion distances around the F^-, Cl^-, Br^- in the crystal structure of **II**, **III**, and **IV** are range 2.6023(11)–3.4682(7), 2.9716(10)–3.4063(10), 3.0037(14)–3.4881(14) Å, respectively, as well as that the mean Ag anion distances are 3.0913(10), 3.2075(10), 3.2906(14) Å. As is mentioned above, the mean Ag–Ag length is $F@Ag_{14} \approx Cl@Ag_{14} < Br@Ag_{14} <$ halogen-free and the analysis of the mean Ag–Ag length and the Ag anion distances reveals that the volume of the cavity of the Ag_{14} cages containing halogen anions also match the tendency of $F@Ag_{14} \approx Cl@Ag_{14} < Br@Ag_{14} <$ halogen-free.

It is obvious that anions in the Ag_{14} cages played a crucial role in determining the volume of these structures [22]. With the increasing of the X^- volume from F^- to Br^-, the Ag_{14} cages are expanded relatively, while the anions shrink the cages overall. As a result, the Ag_{14} cages containing halogen anions are smaller than the halogen-free one, which may be attributed to the electrostatic interaction between the anion and the cationic cage. Though there are reported Ag_{14} cages supported by *tert*-butylethyne [10, 15, 22], these complexes are obviously larger in size, for the steric crowding of the bulky alkynyl ligand. The results have further proved the importance of the anion template.

We also do halogen exchange experiments to investigate the role of the anion template. In the solution of complex **I**, excess $(^nBu_4N)X$ (X = F, Cl, Br) solutions were added, respectively. After evaporation of the mixture at room temperature, complexes **II**, **III**, and **IV** were afforded, which were confirmed by X-ray crystallography and ESI-MS. The results are in consequence with the idea that silver ethnyide cages may undergo a partial disassembly-assembly processes in solutions [23]. However, experiments trying to exchange I^- failed. Upon addition of $(^nBu_4N)I$, white precipitate formed immediately. And attempts to exchange other larger anions, such as CrO_4^- and ClO_4^-, were also failed. The product was shown to be the original complex, since the characteristic absorbance of those

Table 2. The selected Ag anion bond lengths (Å)

	Bond		
	Ag–F	Ag–Cl	Ag–Br
The Ag anion distance in the hexahedron	2.6023(11)	2.9716(10)	3.0037(14)
	2.7960(11)	2.9787(10)	3.0150(15)
	2.9039(12)	3.1469(12)	3.3490(16)
	3.3332(10)	3.3638(10)	3.4285(13)
	3.4440(8)	3.3779(10)	3.4595(14)
	3.4682(7)	3.4063(10)	3.4881(14)
The mean Ag anion distance	3.0913(10)	3.2075(10)	3.2906(14)

anions were not found in the FT-IR spectra. It is mostly because the silver cages were not large enough to hold large anions, for the mean Ag anion bond distance is only slightly more than 3 Å.

Solid state fluorescence spectra of complexes **I–IV** are shown in Fig. 2. These four complexes both have broadband fluorescence emission spectra below 580 nm (λ_{ex} = 300 nm). These emission spectra are probably assigned to metal–ligand charge transfer (MLCT). The highest peaks of complex **I**, **II**, and **IV** are at 450, 443 and 498 nm, respectively, while complex **III** has two emission peaks at 445 and 470 nm. Complexes **II** and **III** have a blue shift of 7 and 5 nm compared with **I**, while complex **IV** has a red shift of 48 nm. It can be associated with the electronic effect of the anions. The withdrawing affection of F^- and Cl^- decrease the electron density of Ag^+ ions, leading to increasing energy of *d* electrons transitions. However, Br^- anions act as electron donators, which increase the electron density of Ag^+ ions and decrease energy of *d* electrons transitions. The different emission shape of complex **III** can be associated with the coordination of THF molecules in the structure, which increase the d^{10}–d^{10} metallophilic contacts.

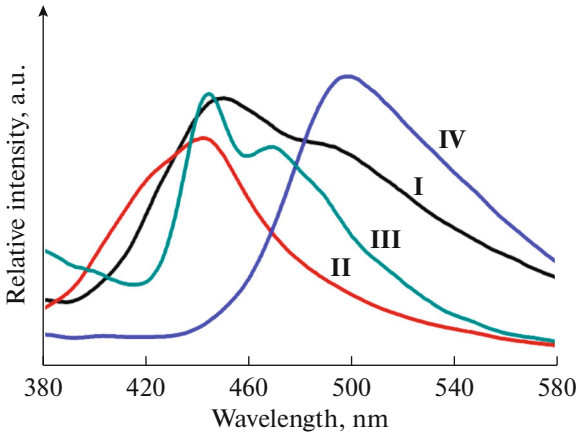

Fig. 2. Solid state emission spectra of complexes **I–IV**.

REFERENCES

1. Wang, Q.M. and Mak, T.C.W., *Angew. Chem. Int. Ed.*, 2001, vol. 40, no. 6, p. 1130.
2. Shahi, S.P. and Koide, K., *Angew. Chem. Int. Ed.*, 2004, vol. 43, no. 19, p. 2525.
3. Pouwer, R.H., Williams, C.M., Raine, A.L., et al., *Org. Lett.*, 2005, vol. 7, no. 7, p. 1323.
4. Halbes-Letinois, U., Weibel, J.M., and Pale, P., *Chem. Soc. Rev.*, 2007, vol. 36, no. 5, p. 759.
5. Yamamoto, Y., *Chem. Rev.*, 2008, vol. 108, no. 8, p. 3199.
6. He, C., Guo, S., Ke, J., et al., *J. Am. Chem. Soc.*, 2012, vol. 134, no. 13, p. 5766.
7. Gao, G.-G., Cheng, P.-S., and Mak, T.C.W., *J. Am. Chem. Soc.*, 2009, vol. 131, no. 51, p. 18257.
8. Xie, Y.P. and Mak, T.C.W., *Angew. Chem. Int. Ed.*, 2012, vol. 51, no. 35, p. 8783.
9. Zhang, Z.Y., Yang, Y., Sun, H.Y., et al., *Inorg. Chim. Acta*, 2015, vol. 434, p. 158.
10. Rais, D., Yau, J., Mingos, D.M.P., et al., *Angew. Chem. Int. Ed.*, 2001, vol. 40, no. 18, p. 3464.
11. Kennedy, A.R., Brown, K.G., Graham, D., et al., *New J. Chem.*, 2005, vol. 29, no. 6, p. 826.
12. Zhao, L. and Mak, T.C.W., *J. Am. Chem. Soc.*, 2005, vol. 127, no. 43, p. 14966.
13. Bian, S.D., Jia, J.H., and Wang, Q.M., *J. Am. Chem. Soc.*, 2009, vol. 131, no. 10, p. 3422.
14. Bian, S.D., Wu, H.B., and Wang, Q.M., *Angew. Chem. Int. Ed.*, 2009, vol. 48, no. 29, p. 5363.

15. Abu-Salah, O.M., Ja'far, M.H., Al-Ohaly, A.R., et al., *Eur. J. Inorg. Chem.*, 2006, vol. 2006, no. 12, p. 2353.

16. Liu, X., Yi, Q.L., Han, Y.Z., et al., *Angew. Chem. Int. Ed.*, 2015, vol. 54, no. 6, p. 1846.

17. Zhang, R., Hao, X., Li, X.M., et al., *Cryst. Growth Des.*, 2015, vol. 15, no. 5, p. 2505.

18. Zhang, R., Zhao, C.Y., Li, X.M., et al., *Dalton Trans.*, 2016, vol. 45, no. 32, p. 12772.

19. Qiao, J., Shi, K., and Wang, Q.M., *Angew. Chem. Int. Ed.*, 2010, vol. 49, no. 10, p. 1765.

20. *APEX2, SADABS, and SAINT*, Madison: Bruker AXS Inc., 2012.

21. Sheldrick, G.M., *Acta Crystallogr., Sect. A: Found. Crystallogr.*, 2008, vol. 64, p. 112.

22. Rais, D., Mingos, D.M.P., Vilar, R., et al., *J. Organomet. Chem.*, 2002, vol. 652, nos. 1–2, p. 87.

23. Connell, T.U., Sandanayake, S., Khairallah, G.N., et al., *Dalton Trans.*, 2013, vol. 42, no. 14, p. 4903.